CellPress

Neuron
Article

Closed-Loop Decoder Adaptation Shapes Neural Plasticity for Skillful Neuroprosthetic Control

Amy L. Orsborn,[1] Helene G. Moorman,[2] Simon A. Overduin,[3] Maryam M. Shanechi,[3] Dragan F. Dimitrov,[4] and Jose M. Carmena[1,2,3,*]

[1]UC Berkeley-UCSF Joint Graduate Program in Bioengineering, University of California, Berkeley, Berkeley, CA 94720, USA
[2]Helen Wills Neuroscience Institute, University of California, Berkeley, Berkeley, CA 94720, USA
[3]Department of Electrical Engineering and Computer Sciences, University of California, Berkeley, Berkeley, CA 94720, USA
[4]Department of Neurological Surgery, University of California, San Francisco, San Francisco, 94143 CA, USA
*Correspondence: jcarmena@berkeley.edu
http://dx.doi.org/10.1016/j.neuron.2014.04.048

SUMMARY

Neuroplasticity may play a critical role in developing robust, naturally controlled neuroprostheses. This learning, however, is sensitive to system changes such as the neural activity used for control. The ultimate utility of neuroplasticity in real-world neuroprostheses is thus unclear. Adaptive decoding methods hold promise for improving neuroprosthetic performance in nonstationary systems. Here, we explore the use of decoder adaptation to shape neuroplasticity in two scenarios relevant for real-world neuroprostheses: nonstationary recordings of neural activity and changes in control context. Nonhuman primates learned to control a cursor to perform a reaching task using semistationary neural activity in two contexts: with and without simultaneous arm movements. Decoder adaptation was used to improve initial performance and compensate for changes in neural recordings. We show that beneficial neuroplasticity can occur alongside decoder adaptation, yielding performance improvements, skill retention, and resistance to interference from native motor networks. These results highlight the utility of neuroplasticity for real-world neuroprostheses.

INTRODUCTION

Brain-machine interfaces (BMIs) create novel functional circuits for action that are distinct from the natural motor system (Carmena, 2013). Motor BMIs map recorded neural activity into a control signal for an actuator via an algorithm (the ''decoder''). Feedback of the actuator movement creates a closed-loop system, allowing the user to modify their behavior in a goal-directed way. Many studies found that the relationship between neural activity and movement changes substantially between natural movements and BMI control (Taylor et al., 2002; Carmena et al., 2003; Ganguly and Carmena, 2009; Ganguly et al., 2011). These changes are likely due in part to key differences between the natural motor and BMI systems, such as different sensory feedback (Suminski et al., 2009, 2010). Increasing evidence also shows that neural activity changes in closed-loop BMI control are related to operant conditioning of neural activity facilitated by biofeedback (Fetz, 2007; Ganguly and Carmena, 2009; Green and Kalaska, 2011; Koralek et al., 2012; Wander et al., 2013).

In closed-loop BMI, biofeedback can facilitate subject learning and substantial performance improvements (Taylor et al., 2002; Carmena et al., 2003; Musallam et al., 2004; Ganguly and Carmena 2009). Moreover, learning to control a BMI can induce neuroplasticity in cortical (Taylor et al., 2002; Carmena et al., 2003; Jarosiewicz et al., 2008; Ganguly and Carmena, 2009; Ganguly et al., 2011; Chase et al., 2012; Hwang et al., 2013; Wander et al., 2013) and corticostriatal (Koralek et al., 2012, 2013) networks. Plasticity has also been associated with the formation of decoder-specific patterns of cortical activity with respect to movement (a ''cortical map'') with properties akin to a motor memory trace (Ganguly and Carmena, 2009). These cortical maps are highly stable, rapidly recalled, and—once formed—resistant to interference from learning other BMI decoders. We refer to these collective properties as ''neuroprosthetic skill,'' reflecting performance and neural representations that are robust over time and resistant to interference. Learning may also facilitate the formation of BMI-specific control networks. Learning-related changes in cortical (Ganguly et al., 2011) and corticostriatal plasticity (Koralek et al., 2013) show specificity for BMI control neurons. The development of skilled BMI control has also been associated with reduced cognitive effort, linked to the formation of a control network distributed broadly across cortex (Wander et al., 2013). Together, this body of work suggests that neuroplasticity may create a specialized BMI control network that allows skillful control.

The robust control attained via neuroplasticity may be particularly useful for neuroprosthetic applications, but several factors could limit the feasibility of such learning in real-world systems. In particular, cortical map formation has been shown to be sensitive to the details of the BMI system, such as the neurons input into the decoder and decoder parameters. Training new decoders regularly, even with the same neural ensemble, eliminated cortical map formation and the associated performance improvements. After a decoder was learned, removing units from the BMI ensemble also led to significantly reduced performance (Ganguly and Carmena, 2009). Consistent with these findings, studies

tracking subjects' performance for weeks to months using daily decoder retraining and nonstable neural ensembles show day-to-day variability in performance (Taylor et al., 2002; Carmena et al., 2003; Musallam et al., 2004; Collinger et al., 2013; Gilja et al., 2012). Maintaining well-isolated, highly stable neural activity for the multiyear lifespan of a neuroprosthesis is infeasible with existing recording techniques; therefore, the ultimate utility of neuroplasticity in these settings is uncertain.

Learning's sensitivity to changes in the BMI system highlights the fact that closed-loop BMI performance is determined by collaboration between the brain and decoding algorithm. Much as neural adaptation has proven beneficial, recent work shows the potential promise of adaptive decoders to improve performance. Closed-loop decoder adaptation (CLDA)—modification of decoder parameters based on closed-loop performance (Dangi et al., 2013)—can reliably improve performance (Taylor et al., 2002; Li et al., 2011; Gilja et al., 2012; Orsborn et al., 2012; Jarosiewicz et al., 2013). CLDA may be particularly useful for compensating for nonstationary neural recordings (Li et al., 2011) and has been shown to produce high-performance BMI control for many months independent of stationary neural recordings (Gilja et al., 2012). Decoder adaptation could potentially be used to facilitate and maintain learning in the presence of changing neural inputs to the BMI. However, relatively little is known about how neural and decoder adaptation might interact, and whether cortical maps can form and be maintained in such a two-learner system. Changing decoder parameters could, for instance, create a ''moving target'' that disrupts formation of stable neural solutions. Early work shows that neural plasticity can occur alongside adaptive decoders (Taylor et al., 2002), but the formation of stable, rapidly recalled cortical maps and BMI-specialized neural circuits in two-learner systems has yet to be explored. Attaining and maintaining neuroprosthetic skill with nonstationary decoders and neural ensembles will be important for the ultimate feasibility of leveraging beneficial neuroplasticity in real-world prostheses.

Beyond changes in neural recordings, real-world neuroprostheses must also be robust to changes in control context. Much like our natural limbs, neuroprostheses will ultimately be used for a myriad of behaviors and in coordination with existing motor and cognitive functions. Tasks that activate brain areas near or overlapping with those used for BMI control, however, may cause performance disruptions. BMI learning and control to date have primarily been studied when subjects control a BMI isolated from other tasks. Learning and associated cortical map formation might be critical for achieving performance that can transfer across contexts.

In this study, we test the feasibility of combining neural and decoder adaptation to achieve and maintain neuroprosthetic skill in two scenarios relevant for real-world neuroprostheses: (1) nonstationary recorded neural activity, and (2) changing control contexts. Two nonhuman primates controlled a two-dimensional cursor using neural activity in motor cortices in the absence of overt arm movements. The stability constraints on neural inputs to the BMI were relaxed by using multi-unit and/or channel-level activity, and the population of units contributing to the decoder was intermittently changed over time. CLDA was used to both improve initial performance of the decoder, and to maintain performance in the presence of nonstationary recordings. We asked whether neuroprosthetic skill would develop in such a system, and explored the interaction between neural and decoder adaptation. To further test the formation of skilled control in this two-learner system and explore the potential benefits of such a skill, we then studied BMI control in a simultaneous BMI and native arm control task. Our findings suggest that leveraging both neural and decoder adaptation may be useful for achieving robust, flexible neuroprosthetic control that can be maintained long term.

RESULTS

To explore whether beneficial neuroplasticity and cortical map formation can occur in a two-learner BMI system, we developed a neuroprosthetic training paradigm to exploit both neural and decoder adaptation (Figure 1A). Our approach used infrequent and minimal CLDA (Figure 1B), interspersed with long periods of fixed decoders. CLDA was used on day 1 to improve initial closed-loop performance. Subsequent practice with a fixed decoder provided the opportunity for neural adaptation and skill consolidation. In the event of a performance drop, or shift in the recorded neural activity (e.g., a unit contributing to the decoder was lost), brief periods of CLDA were used to adjust the decoder (see Table S1 available online and Experimental Procedures).

Emergence of Skilled Neuroprosthetic Performance with Nonstationary Neural Activity and Two Learners

We implemented our CLDA method in two nonhuman primates performing a two-dimensional self-paced delayed center-out reaching task under neuroprosthetic control (Figures 1C–1E, see Experimental Procedures). Subjects were first trained to perform the task with their native arm (manual control, MC) in an exoskeleton. In BMI control, both monkeys performed the task irrespective of overt native arm movement; their arms were positioned outside of the task workspace used for MC. BMI control was implemented with a position-velocity Kalman filter (KF) controlled by small ensembles of multi-unit or channel-level activity (hereafter all referred to as units; see Experimental Procedures). Initial decoders were typically trained using passive observation of cursor movements (see Experimental Procedures). CLDA was performed using the SmoothBatch (Orsborn et al., 2012) or Re-FIT (Gilja et al., 2012) algorithm for monkeys J and S, respectively. Although these CLDA methods are capable of providing high-performance decoders using decoder adaptation alone, initial CLDA was usually performed just until the subject was able to successfully navigate the cursor across the workspace. This allowed ample room for improvement driven by neural adaptation. However, the degree of initial adaptation varied across series (see below).

Task performance showed clear improvements across days in both monkeys (Figure 2A). Cursor trajectories were also refined, with a reduction in the average movement error (Figures 2A and B). CLDA on day 1 substantially improved performance beyond that achieved with the initial decoder. Performance continued to improve after the decoder was held fixed on subsequent days. Intermittent CLDA was able to compensate for performance drops and changes in the neural ensemble, and

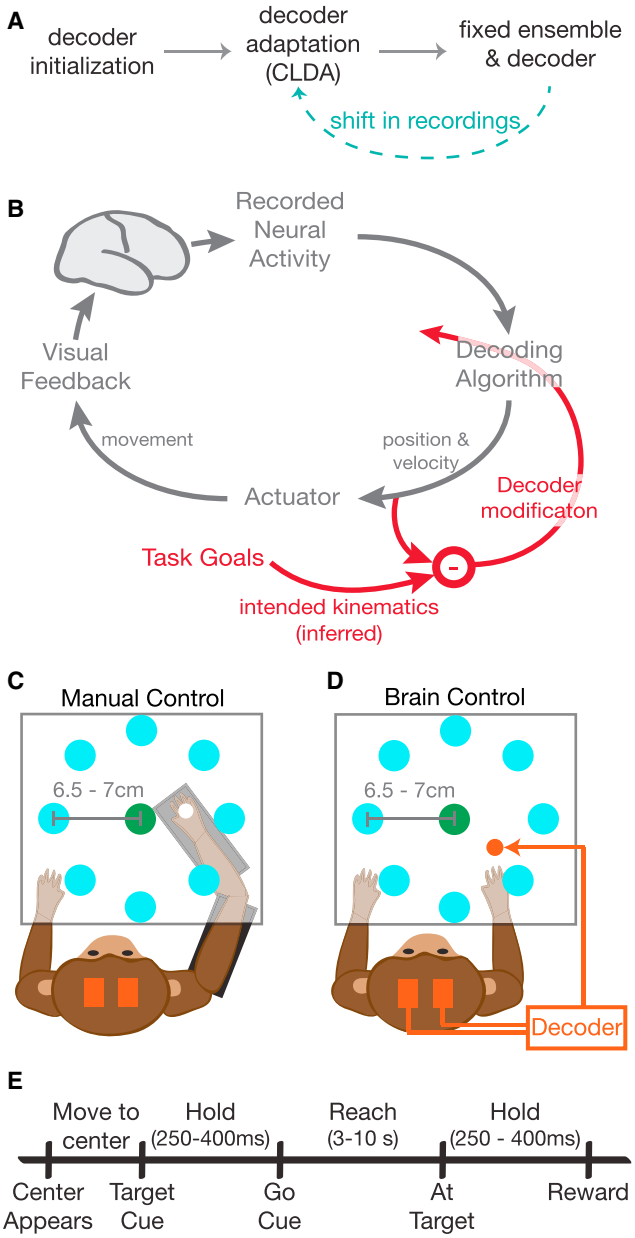

Figure 1. Experimental Setup

(A) Two-learner paradigm for decoder training and performance maintenance. Each series began with an initial decoder, typically trained using visual observation of cursor movements (see Experimental Procedures). CLDA was performed on day 1 to improve performance. The decoder was subsequently held fixed. In the event recorded units in the BMI decoder shifted (e.g., unit lost) or performance dropped, brief periods of CLDA were performed.

(B) Schematic illustration of CLDA. CLDA modifies the decoder parameters during closed-loop BMI control. The closed-loop BMI system is illustrated in gray; decoder modification is shown in red.

(C and D) Two monkeys were trained to perform a two-dimensional self-paced, delayed center-out movement task in both manual control (C) and brain control (D). In brain control, the subject's arm was confined within a primate chair.

(E) Timeline of the center-out task. See Experimental Procedures for details.

performance improvements continued after midseries modifications. Subjects also showed intraday learning that was retained across days (Figure 2C). That is, there was little to no re-learning on days when the decoder was held static with a stable neural ensemble. These trends held across multiple series performed by both subjects (Figure 2D). A comparison of performance on day 1 (after initial adaptation; "Early") with the maximum performance achieved during the series ("Late") shows significant improvements in all behavioral measures (one-sided Wilcoxon signed rank test; $p < 0.05$).

Importance of Decoder Stability and Specificity of Learning

Subjects showed gradual refinement of cursor control, with continued improvements in movement errors and success rates even after task success (percent correct) reached a plateau (Figure 2A). These improvements were absent when CLDA was used each day to maximize performance starting from varying initial decoders that used differing neural ensembles. Whereas CLDA could achieve high task performance, movement kinematics showed no improvements (Figures S1A and S1B). Daily performance also showed variability commonly observed with daily retraining (e.g., Taylor et al., 2002; Carmena et al., 2003; Musallam et al., 2004; Collinger et al., 2013; Gilja et al., 2012).

This finding confirms that observed learning was not purely reflective of increased practice in BMI and highlights the importance of some degree of neural and decoder stability for learning. However, there are several possible explanations for the lack of learning with daily CLDA. These experiments not only applied CLDA more often, but also made more abrupt decoder changes day-to-day (by retraining from a new seed daily) and varied the neural ensembles. Alternately, CLDA may saturate performance, making additional improvements infeasible. To better understand these factors, we ran an additional experiment with monkey J where CLDA was run continuously each day starting from the previous day's parameters with a semistationary neural ensemble (see Supplemental Experimental Procedures). The subject showed gradual performance improvement (Figure S1E), suggesting that frequent CLDA, in and of itself, may not disrupt learning. It also further shows the potential for performance improvements beyond that attained by initial CLDA. These findings imply that a two-learner BMI might achieve higher performance than CLDA or neural adaptation alone.

Finally, to further verify that learning was decoder specific, we tested performance with novel decoders with monkey J. Closed-loop performance dropped significantly when using unpracticed test decoders (Figures S1C and S1D). Similar to previous studies (Ganguly and Carmena, 2009), these perturbations were reversible and high levels of performance quickly returned when learned decoders were reinstated.

Neural Adaptation and Map Formation in a Two-Learner BMI

We next explored neural activity underlying task improvements and robust recall of performance. The directional tuning of units contributing to the BMI cursor was assessed each day within learning series (see Experimental Procedures) to determine how the relationship between cursor movement and neural

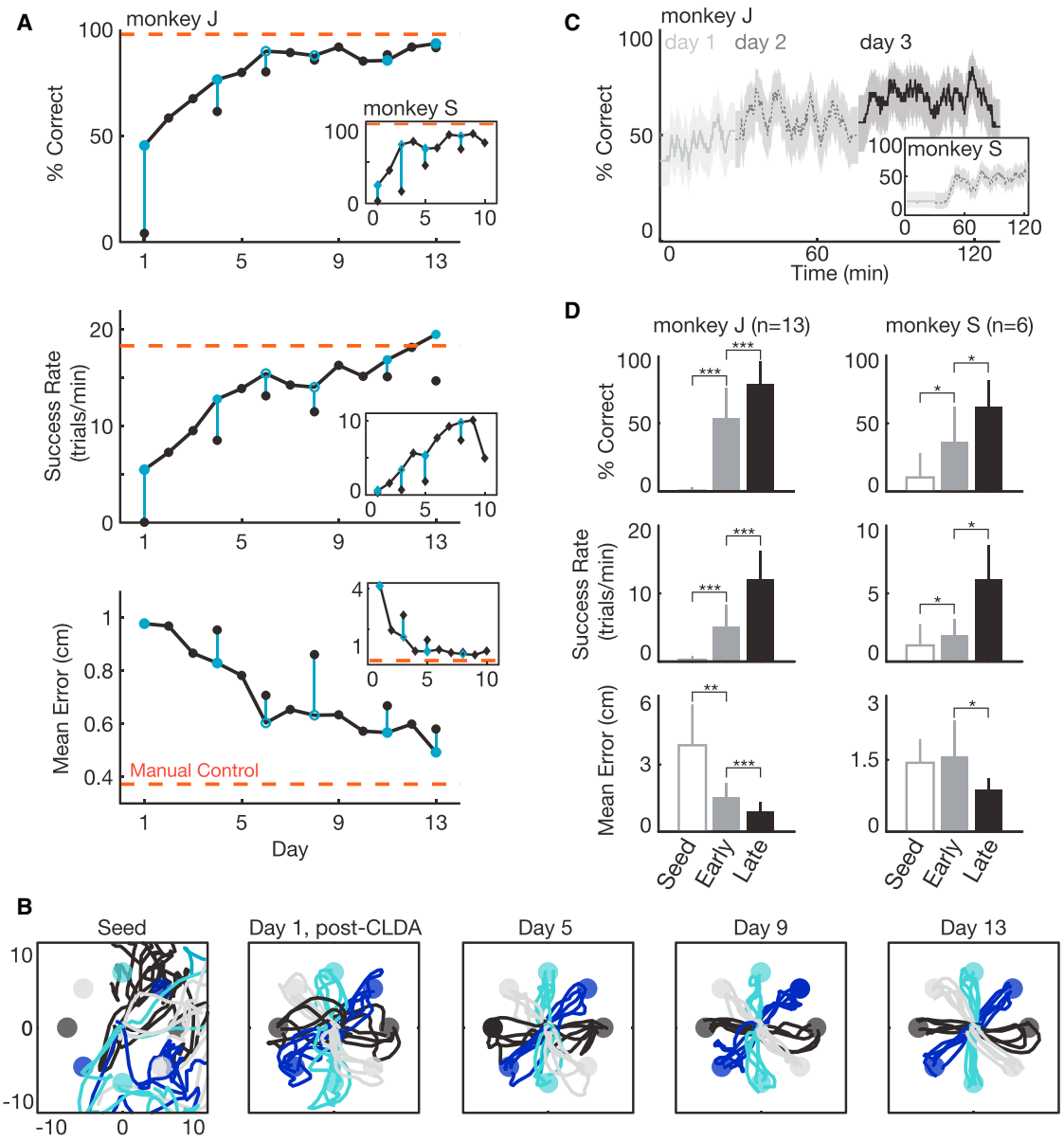

Figure 2. Behavioral Performance in a Two-Learner BMI System

(A) Example learning series for monkeys J (main) and S (insets), quantified by task percent correct, success rate, and movement error. Blue indicates when CLDA occurred, and open circles indicate times when CLDA was used to swap units in the decoder. Orange lines show typical performance with arm movements (manual control) for each animal.

(B) Randomly selected reach trajectories over days for the example learning series from monkey J shown in (A). Five trajectories per target are shown, excluding the Seed condition, where control was too poor to produce sufficient reaches. Colors denote different reach directions; scale is in centimeters.

(C) Sliding average (50 trial window) of task performance for days 1–3 (monkey J) and 1–2 (monkey S) in the example series shown in (A). Shading indicates 95% CI (Agresti-Coull binomial CI). The decoder was held fixed over these days, after initial CLDA on day 1. Sliding averages were done separately for each day.

(D) Average improvement over all learning series (n = 13, monkey J; n = 6, monkey S) for task percent correct, success rate, and movement error (see Experimental Procedures). "Seed" shows the performance with the initial decoder. "Early" corresponds to performance on day 1 following CLDA. "Late" corresponds to the best performance achieved after day 1. Bars represent means; error bars represent SD. *p < 0.05; **p < 0.01; ***p < 0.001, one-sided, paired Wilcoxon sign-rank test.

activity changed over time. Figures 3A–3C show cosine tuning curve fits for three example units for 4 days within a learning series. Unit tuning properties (modulation depth and preferred direction; subsequently denoted as MD^U and PD^U, respectively) changed gradually over the course of a series for the majority of units within the ensemble (Figure 3D).

To quantify learning-related neural tuning changes at the population level, we performed a direction tuning map analysis

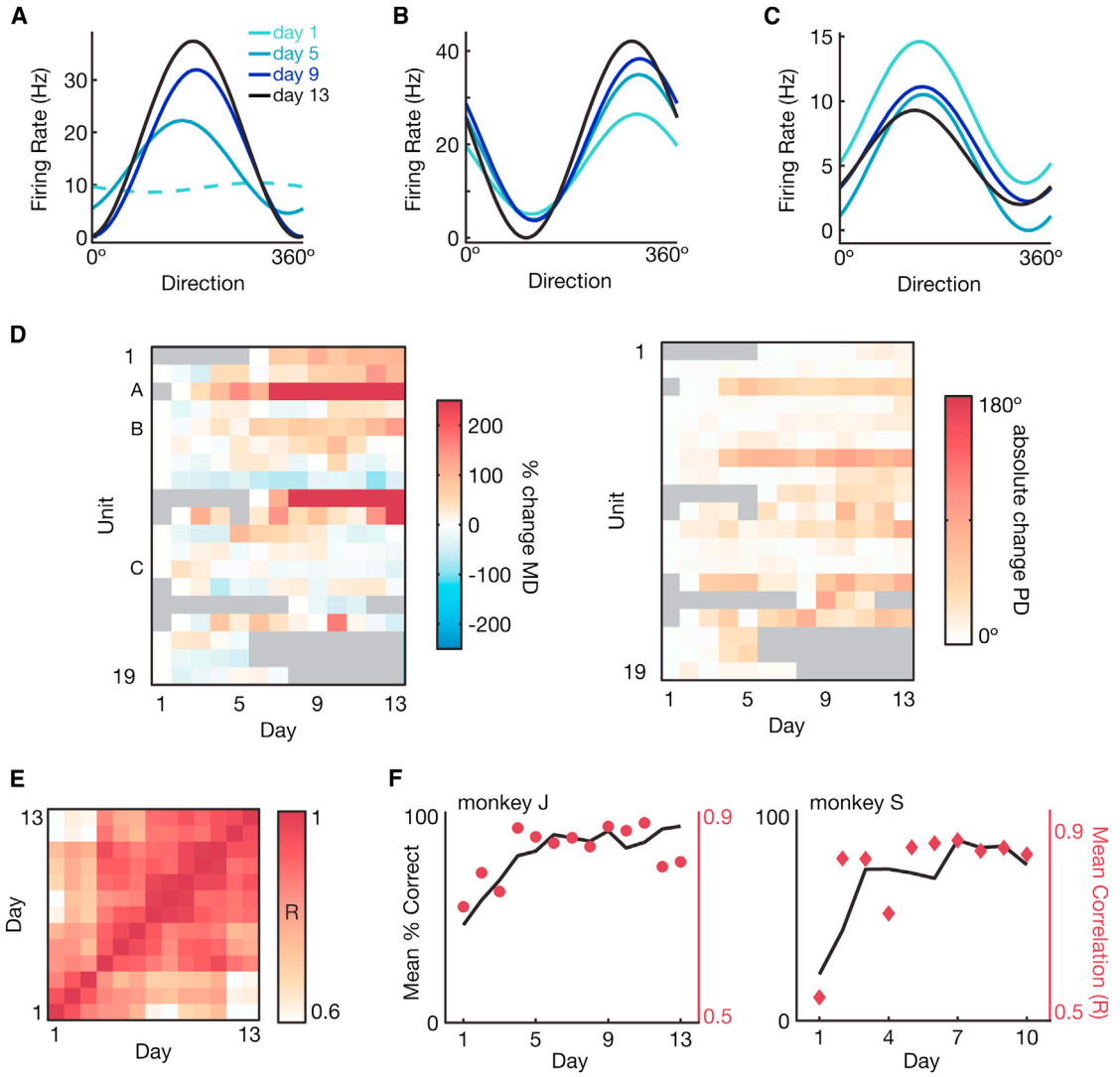

Figure 3. Neural Tuning Changes and Map Consolidation

(A–C) Fitted tuning curves for sample units across days within a decoder series. Data are from monkey J for the 13-day decoder series shown in Figure 2A. Color indicates the day (light to dark progression); dashed lines represent nonstatistically significant tuning fits.

(D) Changes in tuning modulation depth (MD^U) and preferred directions (PD^U) for all BMI units across the decoder series (relative to the first day). Units were sorted by the strength of modulation on the final day (in descending order). Grey squares indicate units that were not part of the ensemble, or were not significantly tuned.

(E) Pairwise correlations of the ensemble tuning maps across the decoder series (see Experimental Procedures).

(F) Average map correlation for each day (red) overlaid onto task percent correct (black). Examples are shown for the series from monkey J and monkey S shown in Figure 2A.

(Ganguly and Carmena, 2009). The fitted tuning curves for the BMI ensemble for each day form a cortical map. We performed pairwise correlations among the daily maps within a learning series (see Experimental Procedures). Maps were more strongly correlated to one another late in learning, showing the stabilization of a neural representation (Figure 3E). The average correlation of each day's map with all others, which reflects the degree of map stability, increased late in learning, with a time course very similar to the task performance improvements (Figure 3F). Similar changes and stabilization of unit activity were also observed when continuous CLDA was performed (Figures S1F–S1K).

Together, these behavioral and neural results show that beneficial neuroplasticity can occur with semistationary BMI circuits. Moreover, both performance improvements and cortical map formation were not sensitive to midseries changes in the BMI ensemble. Recorded units were only partially stationary, showing slight variability in waveforms and firing properties during native arm movements (Figure S2). Cortical maps computed in arm movement and visual observation tasks did not show stabilization trends for monkey J (Figures S2A–S2C), suggesting that the emergence of a stable map in BMI control cannot be attributed to this recording variability. Furthermore, cortical

map stability and behavioral improvements were not impeded by small ensemble membership changes (Figure S2H).

Degree of Neural Adaptation Depends on Amount of Performance Improvements

Little is known about how learning might be distributed across a two-learner BMI system. We thus examined the relationship between neural and decoder adaptation. We hypothesized that stable neural representations would form regardless of the initial amount of CLDA, but that the degree to which the subject improved performance after initial CLDA would influence the degree of neural adaptation. The amount of improvement after initial CLDA varied across series. Figure 4A shows example map correlations for series in which performance improved by different amounts after initial CLDA, or no CLDA was used. Series with low initial performance showed gradual improvement. Performance was readily maintained in those series with high performance achieved with CLDA on day 1. Interestingly, neural maps showed signs of gradual stabilization for all series, regardless of the amount of initial CLDA. However, the amount of change in the neural map over the course of the series (as approximated by average map correlation) differed across series, mirroring the behavioral performance. To quantify this effect, we compared the amount of behavioral performance improvements attained in a series (maximum performance attained in a series compared to day 1 post-CLDA) to the degree of population-level neural adaptation. Across all series ($n = 14$, pooling subjects and limiting analyses to series with 2 days or longer of stable decoder practice; see Experimental Procedures), task performance improvements and the average similarity of the initial tuning map with subsequent days were significantly correlated (Figure 4B; $R = -0.8$, $p < 0.0007$).

We then quantified the changes in the units' directional tuning properties as a function of behavioral improvements. Changes for each unit were quantified by comparing its tuning properties early and late in the series (defined by behavioral criteria; see Experimental Procedures); unit changes were then averaged across the BMI ensemble. All series showed some degree of tuning changes in both modulation depth (MD^U) and preferred direction (PD^U). The magnitude of these changes, however, varied depending on the amount of improvement in task percent correct attained in the series (Figure 4C; MD^U: $R = 0.84$, $p < 0.0002$; PD^U: $R = 0.67$, $p < 0.009$). MD^U changes were also significantly correlated to other measures of behavioral improvement, including cursor kinematics (Table S2). PD^U changes were only related to improvement in task-level metrics (percent correct; success rate). The proportion of units within the BMI ensemble showing statistically significant tuning changes was also related to behavioral improvements. Units fell into four categories: no change, change in PD^U or MD^U only, and both MD^U and PD^U changes. All four types were observed, but the proportions of each category varied with the amount of behavioral improvement (Table S2). Strikingly, the fraction of the ensemble with changes in both MD^U and PD^U was strongly correlated with task improvements (Figure 4D; $R = 0.74$, $p < 0.004$). More units substantially changed directional tuning (with changes in both properties) when large performance improvements were required. In series where performance improvements were smaller, units either showed no change, or only modified a single aspect of their tuning. Neural ensemble activity in the series with continuous CLDA was also consistent with this trend, showing highly stable map activity (Figures S1F and S1G) and tuning changes dominated by MD shifts (Figures S1H–S1K).

Neural Adaptation Is Shaped by Decoder Properties

Our results suggest that neural tuning properties changed primarily when necessary to improve performance and were otherwise stable. In a BMI system, performance is determined by both the neural activity and decoder. Neural tuning changes, then, might be shaped by properties of the decoder. We investigated whether properties of the KF decoders trained with CLDA influenced neural adaptation on subsequent days. The KF models the relationship between the cursor state (Cartesian position and velocity) and neural activity using a linear relationship described by the matrix C (see Experimental Procedures). This model can be interpreted as assigning independent position and velocity directional tuning to each unit. We computed the position and velocity MD and PD of each unit assigned by the decoder (MD^{C_p}, MD^{C_v}, PD^{C_p}, and PD^{C_v}, respectively; see Experimental Procedures), and asked how these properties related to unit tuning changes (Table S3). Units were more likely to increase MD^U if they were assigned a larger decoder MD (MD^{C_v}) (Figure 4E, $R = 0.26$, $p < 10^{-4}$). Similarly, the amount of mismatch between a unit's PD (PD^U and that assigned by the initial decoder was correlated with changes in PD^U within the series (Figure 4F, $R = 0.22$, $p < 10^{-4}$). That is, units were more likely to change their preferred directions if the initial decoder assigned them an "incorrect" PD. Together, these results show that unit tuning changes were shaped, in part, by the decoder.

Refinement of Neural Activity Temporal Recruitment

The above analyses suggest that neural adaptation might partly be used to refine neural recruitment to best match the decoder properties. One unexplored question is whether plasticity might also influence the temporal recruitment of neural activity in BMI control. Figure 4G shows poststimulus time histograms for two example units early, mid, and late within a decoder series. In addition to increases in maximum firing rate, these units show a temporal shift in recruitment with learning. We calculated the onset time of directionally tuned activity and time of peak firing (see Experimental Procedures) for each unit early and late in learning. Averaging across all units and series, we found that after learning, units were both directionally tuned earlier and reached peak firing earlier in the trial (Figure 4H, paired Wilcoxon sign-rank tests, $p < 10^{-5}$ and $p < 10^{-4}$ for both subjects, respectively). Note that time is defined relative to cue for movement initiation ("go-cue"). The majority of units developed tuning prior to the go-cue (negative times), which could indicate planning or preparation to move. However, we found that cursor speed profiles also shifted earlier with learning, and clear increases in speed occurred prior to the go-cue (Figure S3). The negative times therefore more likely reflect reach initiations launched prior to the go-cue. These results show that in addition to changes in tuning properties, learning can induce changes in the temporal recruitment of neurons.

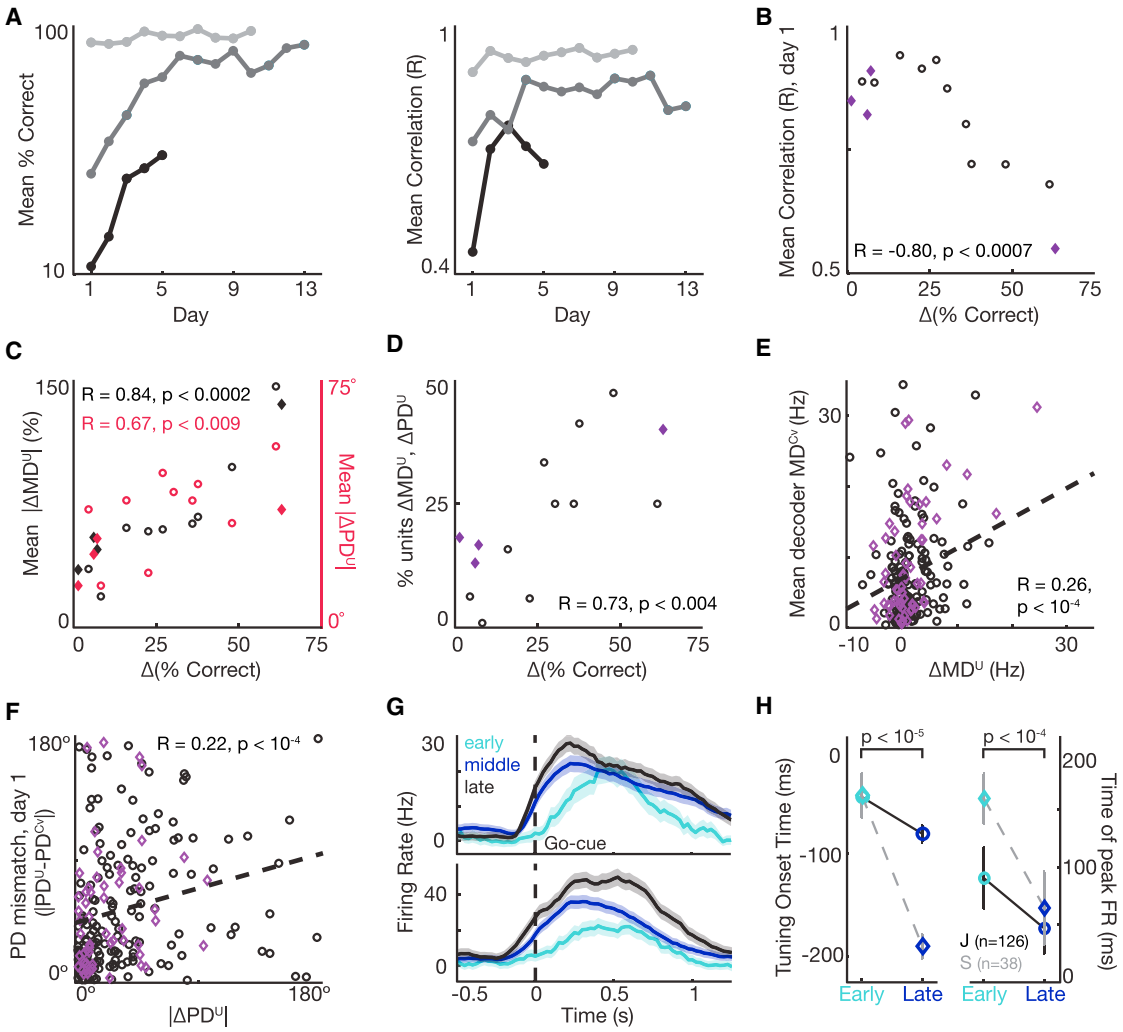

Figure 4. Degree of Neural Adaptation Depends on Amount of Performance Improvement

(A) Mean neural tuning map correlations (see Experimental Procedures and panels E and F) for three example series with different degrees of performance improvement (and amounts of CLDA). Task performance for corresponding series is shown at left. Note that the black trace is from a series with a Wiener filter decoder where no CLDA was performed (series not included in subsequent analyses due to different methodology but included here for illustrative purposes).

(B) Mean map correlation on day 1 plotted as a function of the change in task success for all series. Black circles and purple diamonds represent monkey J and S data, respectively.

(C) The ensemble-averaged change in modulation depth (ΔMD^U; black) and preferred direction (ΔPD^U; red) as a function of the change in task success for all series. Circles and diamonds represent monkey J and S data, respectively.

(D) The fraction of BMI units with statistically significant changes in both PD^U and MD^U as a function of task performance improvements.

(E) Change in MD^U versus the average decoder weight (MD^{CV}, see Experimental Procedures) assigned to a unit. Format as in (B). Black line represents linear regression.

(F) Magnitude of change in PD^U during learning compared with the initial angular error in the decoder PD. Format as in (B). Black dashed line shows linear regression.

(G) Poststimulus time histogram aligned to the go-cue of sample units across learning. Firing rates for each example unit are shown for reaches in the unit's preferred direction early (light blue), mid (blue), and late (black) in learning. Solid lines represent the mean; shading represents SEM. Data are from the 13-day series illustrated in Figure 2A for monkey J.

(H) Time of directional tuning onset (left) and time of peak firing rate (right) for individual units early and late in learning. The average across all units for monkeys J (circles) and S (diamonds) is shown early (light blue) and late (dark blue) in learning. Error bars represent SEM. Timing is defined relative to the go-cue.

Neural Adaptation Reduces Interference from Native Motor Networks

Behavioral and neural analyses suggested that the two-learner paradigm facilitated performance improvements that were rapidly recalled with corresponding stabilization of neural representations. Furthermore, this neuroprosthetic skill formation may occur even when CLDA is used to substantially improve initial performance. To further confirm the formation of neuroprosthetic

skill, and to explore the potential benefits of such skill for real-world neuroprostheses, we tested the emerging neural map's resistance to interference from exposure to other contexts and perturbing neural inputs. In particular, we explored resistance to interference from native motor networks. Such resistance may be critical for coordinating neuroprosthetic control with residual motor functions. We hypothesized that the neural activity evoked by overt arm movements during BMI operation would significantly disrupt BMI performance due to recruitment of overlapping neural networks. We predicted that skilled control of the BMI in isolation ("BMI-only" context) would be resistant to BMI training in a second context (i.e., in the presence of native arm movements). Moreover, we theorized that neuroplasticity and skill formation might be critical for reducing disruptions from native motor networks.

We developed a behavioral paradigm which required the subject to simultaneously control his arm and the BMI cursor ("simultaneous control," or BMI-SC; Figures 5A and 5B). The subject performed an isometric force task with the arm contralateral to the majority of units used for BMI decoding while also performing a center-out task with the BMI cursor (see Experimental Procedures). Monkey J performed the BMI-SC task intermittently during a BMI decoder series (n = 5 series). Note that the subject used the same decoder in BMI and BMI-SC control. As expected, the isometric force task significantly disrupted BMI performance (Figure 5C). However, BMI-only performance and learning was not disrupted by performing the BMI-SC task with the subject showing marked performance improvements (Figure 5D; one-sided paired Wilcoxon signed-rank test; $p < 0.05$). Sessions in which the subject performed BMI and BMI-SC in an A-B-A block structure also showed minimal within-session interference between contexts (Figure S4).

While exposure to the BMI-SC task did not disrupt learning in the BMI-only context, the simultaneous force task did significantly reduce the subject's ability to operate the BMI. We examined how neural activity differed between contexts to test whether this disruption was due to interactions between neural networks. Unit directional tuning was typically perturbed in BMI-SC control relative to BMI, with changes in both MD^U and preferred direction PD^U (Figure 5E). Interestingly, PD^U perturbations were evenly distributed across units (i.e., no net rotation; ΔPD^U distributions not significantly different from 0, whereas $|\Delta PD^U| > 0$; Wilcoxon sign-rank tests). This was evident both when pooling across series, and within individual BMI ensembles for each series. MD^U changes, in contrast, were biased, with units modulating significantly less in BMI-SC relative to BMI-only (Wilcoxon signed-rank test). Native arm movements thus disrupt BMI performance by perturbing the BMI neural map.

Strikingly, BMI-SC performance also improved across the series, approaching that of BMI-only performance on the last day in one example (Figure 5C). On average, BMI-SC performance markedly improved within each series (although not statistically significant; one-sided paired Wilcoxon sign-rank test; Figure 5D). Performance in BMI-SC over the full course of training, however, showed no significant correlation with time (percent correct: $R = 0.5$, $p = 0.12$; success rate: $R = 0.14$, $p = 0.69$). This suggests that within-series improvements were not purely due to increasing familiarity with the BMI-SC paradigm. Another possibility is that interference from native motor networks might be reduced as neuroprosthetic skill formed within a decoder series. To test this alternative hypothesis, we quantified changes in neural map perturbations over learning. Figure 5F shows fitted tuning curves for two example units during BMI-only and BMI-SC early and late in learning. Tuning in BMI-SC late in learning often changed to shift closer to that of BMI-only. We quantified this effect at a population level by computing the difference in a unit's MD^U and PD^U in BMI-only and BMI-SC each day. Comparing the difference in tuning properties early and late in learning, we found a significant reduction in PD^U perturbations (paired Wilcoxon signed-rank test, $p < 0.03$), but no significant change in the magnitude of MD^U perturbations (Figure 5G).

DISCUSSION

Together, these results demonstrate the feasibility of combining decoder and neural adaptation to produce robust neuroprosthetic performance that can be maintained despite nonstationary neural inputs and changes in context. Daily recall of performance was accompanied by the formation of stable cortical maps, and performance improvements were driven by changes in units' relationships to cursor movement. Relationships between neural and decoder adaptation also suggest that CLDA might help shape neural activity during closed-loop BMI control and learning. Critically, stable performance and neural representations developed even when the majority of performance improvements were achieved via decoder adaptation. Neuroprosthetic skill development showed resistance to interference from practicing BMI in other contexts and may also increase the BMI ensemble's resistance to perturbing inputs.

Relationship between Decoder Stability and Neural Adaptation

Previous results suggest that neuroprosthetic skill formation is strongly tied to stability of the BMI decoder and ensemble (Ganguly and Carmena, 2009). Our results expand this finding to suggest that skill formation can still occur in the presence of gradually changing decoder parameters and ensembles. The smooth, gradual nature of our decoder and ensemble changes may be critical for facilitating skill formation. Exploration of coadaptive learning in human-machine interfaces suggests that machine learning algorithms that make more gradual decoder modifications may be easier for subjects to learn (Danziger et al., 2009). The same may be true in BMI. Although the decoder was allowed to adapt in our paradigm, we found that after initial CLDA training, further decoder adaptation produced relatively conservative changes in parameters over the course of a series (Figures S2I–S2K). Changes in the BMI ensemble were also made gradually, with approximately 10% of the ensemble (1–2 units) changing at a time. The importance of gradual decoder adaptation for skill formation is further supported by the varied learning rates found in studies with daily decoder retraining, with or without CLDA, where decoder properties and BMI ensembles are more abruptly changed (Figure S1, also Taylor et al., 2002; Carmena et al., 2003; Musallam et al., 2004; Gilja et al., 2012; Collinger et al., 2013).

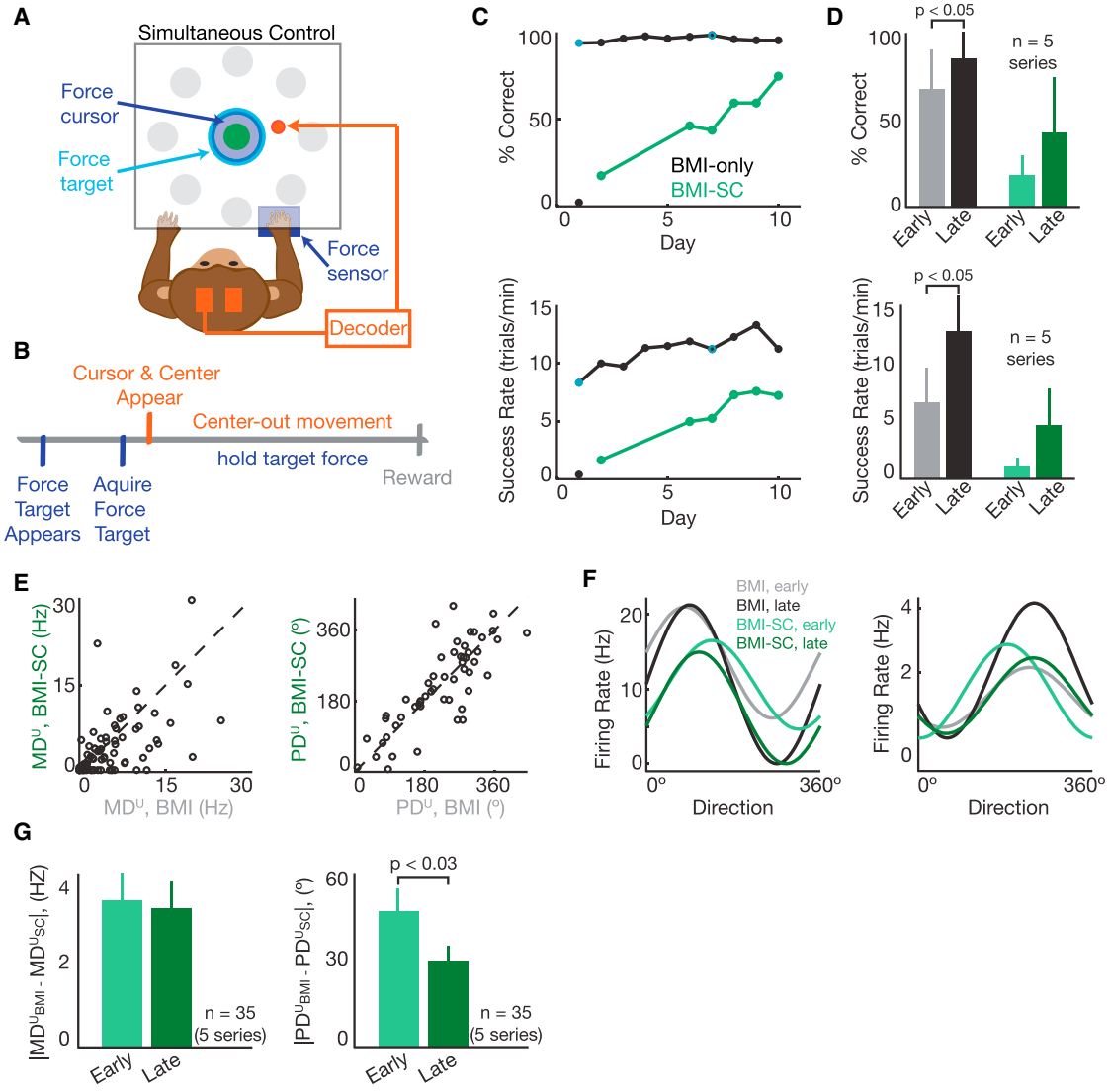

Figure 5. Resistance to Interference from Native Arm Movements

(A and B) Monkey J performed a simultaneous control (BMI-SC) task. He performed an isometric force generation task using his right arm to apply force to a sensor. Force feedback and force targets were displayed via a force cursor (dark blue) and a target ring (force target; light blue). In BMI-SC, the subject acquired a force target, triggering the appearance of the BMI cursor and center-out task, and then performed a center-out reach with the BMI cursor while maintaining the applied force.

(C) Performance (percent correct trials, top; success rate, bottom) for an example series in which the subject performed the center-out task in BMI (BMI-only) daily with intermittent BMI-SC blocks. Black represents BMI-only performance (blue represents when CLDA was applied); green represents BMI-SC performance.

(D) Average BMI-only and BMI-SC task performance (percent correct and success rate), early and late for five decoder series. Error bars represent SD.

(E) Comparison of units' directional tuning parameters (MD^U, left; PD^U, right) in BMI-only and BMI-SC on the first day of BMI-SC control across all series.

(F) Fitted tuning curves for two example units during BMI-only (gray, black) and BMI-SC (light and dark green). Tuning curves early and late are shown for both task conditions.

(G) Comparison of the tuning properties (MD^U and PD^U) in BMI-only and BMI-SC early and late in learning. Bars represent the mean; error bars represent SEM. Differences were only defined for units that were significantly tuned across both tasks, both early and late, reducing the population to 35 units (of 78).

Interestingly, we found that continuous CLDA with semistationary neural ensembles can also produce learning (Figures S1E–S1K). This adaptation method also made relatively small changes to decoder parameters over time (see Supplemental Experimental Procedures), but more frequently (both in the timescale of CLDA and frequency of CLDA application; Shanechi and Carmena, 2013). Additional research is needed to fully explore the timescales of CLDA and the degree of neural ensemble stability required to optimize skill formation. Full understanding of the interactions between neural and decoder adaptation will both inform design of new CLDA algorithms (Dangi et al., 2013) and procedures for maximizing performance for neuroprosthetic

applications. Our results provide evidence that it may be both feasible and advantageous to leverage neural and decoder adaptation in neuroprosthetic applications.

Neural Adaptation Mechanisms in BMI

Our results show that a two-learner system can facilitate performance improvements partially driven by changes in the BMI ensemble units' firing properties. We observed changes in units' modulation depth and preferred directions, consistent with previous findings (Taylor et al., 2002; Carmena et al., 2003; Jarosiewicz et al., 2008; Ganguly and Carmena, 2009; Ganguly et al., 2011; Chase et al., 2012; Hwang et al., 2013). These properties may be somewhat independent of one another, with many units showing either changes in MD or PD alone. Both MD and PD changes were linked to the decoder properties (Figures 4E and 4F). These results suggest that MD changes may be driven by "credit-assignment" processes to increase modulation of units most strongly linked to cursor movements, whereas PD changes are driven by mismatch between the cursor movement and the subject's intent. These findings are consistent with evidence that BMI skill learning gradually shapes network activity by selectively modulating BMI units (Ganguly et al., 2011), and that subjects can selectively rotate PDs of individual units within the BMI ensemble (Jarosiewicz et al., 2008; Chase et al., 2012).

Importantly, the amount of neural adaptation varied with decoder adaptation (Figure 4). This provides further evidence that neural adaptation is shaped by errors provided during closed-loop control. Neural activity, however, still showed changes even when initial CLDA provided the subjects with a decoder with minimal errors. These changes were primarily restricted to units' MDs (Figures 3A–3D, 4C, 4D, and S1H–S1K). Previous work suggests that MD changes in BMI learning may reflect the formation of a BMI-specific control network (Ganguly et al., 2011). MD changes in our two-learner system, then, may reflect similar neural adaptation processes. Even when CLDA provides subjects with decoders that approximate their intentions, neural adaptation may be critical for shaping the neural circuit contributing to cursor movements. This is consistent with the observed changes in neural recruitment timing with learning (Figures 4G and 4H). Such changes may also reflect learning of an internal model of the BMI system (Golub et al., 2012). Formation of BMI-specific networks is closely related to our findings on resistance to interference observed with learning, as discussed below.

While our results show that neural tuning changes were tied to decoder properties and behavioral performance, these factors did not completely explain observed neural changes. For example, preferred direction changes and decoder parameters were significantly correlated, but only weakly so. This may be due in part to incomplete subject learning, or could suggest that neural solutions used in BMI are constrained as has been suggested by Hwang et al. (2013). It is currently unknown whether, for instance, neural ensemble selection may influence plasticity. The differences in amount and type of neural adaptation observed across series in our study could be due in part to properties of the selected BMI ensemble. Ensemble-level constraints, however, cannot fully explain our observations given the many significant relationships among tuning changes, decoder properties, and behavior. Identifying the mechanisms driving learning in BMI and the limitations of learning is an important remaining challenge (Green and Kalaska, 2011, Jackson and Fetz, 2011).

BMI Network Formation and Resistance to Interference from Native Motor Networks

Our results suggest that, even when CLDA provides the subject with a highly performing initial decoder, neural adaptation facilitates the formation of a BMI-specific network (Ganguly et al., 2011). Previous work suggested that such learning was resistant to interference. Subjects were able to learn multiple BMI decoders with the same neural ensemble and retain each in memory (Ganguly and Carmena, 2009). Here, we broaden these results to show in one subject that BMI skill formation was resistant to interference from controlling a BMI in different contexts (with and without simultaneous arm movements; Figure 5). Skill formation in the BMI-only context was not disrupted by performing the simultaneous control task. These results also provide further evidence that neuroprosthetic skill can form with combined neural and decoder adaptation.

We also find that learning might reduce the context-dependence of BMI control. BMI-SC performance improved late in the decoder series, even with little or no additional practice in the BMI-SC context. Our results cannot rule out the possibility that the subject learned two different BMI-control contexts independently (i.e., that improvements in BMI-SC control are separate from BMI-only skill formation), nor can we fully exclude the possibility of general learning of the BMI-SC task. However, neural activity during BMI-SC was more similar to that of BMI-only late in learning, suggesting that BMI-SC improvements may be due in part to reduced interference of arm-movement-related activity with BMI control. Neural perturbation reductions were only significant for PD changes. Thus, the disruption of simultaneous arm movements may not be fully blocked by skill formation.

Additional studies exploring long-term BMI learning in multiple contexts are needed to fully explore these effects. The potential for intersubject variability should be considered when interpreting our results, and studies using larger subject pools will be necessary. Moreover, allowing subjects to practice in a single context (e.g., BMI-SC) for a prolonged period before being exposed to a second context (e.g., BMI-only) might be particularly useful for understanding the degree of learning transfer between contexts. The degree of disruption between context changes may also depend on the contexts' functional similarity. Electroencephalographic BMI studies suggest that performance of simultaneous cognitive tasks impacts control, but only marginally (Foldes and Taylor, 2013). Simultaneous motor tasks involving overlapping neural ensembles, such as the BMI-SC tested here, may be more disruptive. Further study of the mechanisms underlying BMI learning—such as structural and functional changes in the BMI ensemble and up- and downstream areas—are also needed to understand if and how skill formation might reduce network interference and increase resistance to perturbations. Deeper understanding of how neural plasticity shapes resistance to interference from competing

neural networks will be critical for developing robust, flexible neuroprostheses.

Implications for Neuroprostheses

Our results demonstrate the potential importance of neural plasticity for neuroprosthetic applications. Neural plasticity can provide performance that is reliably recalled over days, and resistant to interference from native motor networks. Moreover, we show that it is feasible to use combined neural and decoder adaptation to attain these beneficial properties even in the presence of real-world limitations such as nonstationary neural recordings and poorly conditioned initial decoding algorithms. Such two-learner approaches may be useful for clinical applications. By using decoder adaptation to improve initial performance, learning times might be reduced, providing users with a functional device immediately. Similarly, CLDA could be used to compensate for gradual shifts in neural recordings to reduce recording stability requirements without significantly disrupting learning. However, additional research is needed to identify the training paradigm that optimizes long-term neuroprosthetic performance. Our results demonstrate that neuroprosthetic skill can develop even in the presence of gradual decoder and neural ensemble changes. Furthermore, we found that performance improved even when CLDA was used to fully adapt the decoder, suggesting that neural plasticity may provide benefits beyond decoder adaptation alone. Whether two-learner approaches yield better performance than paradigms primarily using decoder or neural adaptation alone is an important question for future study.

Two-learner approaches also open possibilities for shaping long-term BMI performance. The interactions between CLDA and neural adaptation we observed could potentially be leveraged to guide neural solutions toward optimal strategies (Merel et al., 2013). This could be particularly important for systems with many degrees-of-freedom, where the manifold of possible control solutions becomes complex and could contain many singularities and local maxima. Gradual adaptation, of both the decoder and subject, might be a useful tool to guide the system to maximal performance. Such approaches may be highly effective because our findings suggest the brain can effectively pick-up where the decoder leaves off. A gradual training approach where control complexity gradually increases has already proven useful in multi-degrees-of-freedom neuroprosthetic control (Velliste et al., 2008; Collinger et al., 2013). Combining this method with the two-learner decoder training paradigm developed here may be particularly fruitful. Comparison studies will be needed to identify the most effective training paradigm.

Finally, the demonstration of reduced interference from native motor networks with skill formation may be critical for real-world applications. Ultimately, neuroprostheses will be used outside of a lab setting, where patients will control their devices in coordination with residual motor functions and while performing other cognitive tasks. Here, we show that these changes in context may be highly disruptive. However, learning can be used to overcome these disruptions, either by allowing users to learn and retain multiple context-specific BMI solutions, or by forming a BMI-specific network resistant to interference from external perturbations.

EXPERIMENTAL PROCEDURES

Surgical Procedures

Two male rhesus macaques (*Macaca mulatta*) were chronically implanted with arrays of 128 microwire electrodes. Arrays were implanted bilaterally targeting the arm area of the primary motor cortex (M1). See Supplemental Experimental Procedures for further details. All procedures were conducted in compliance with the NIH Guide for the Care and Use of Laboratory Animals and were approved by the University of California, Berkeley Institutional Animal Care and Use Committee.

Electrophysiology

Neural activity was recorded using a 128-channel MAP system (Plexon). For this study, multi-unit (monkey S) and channel-level (monkey J) activity was used. Multi-unit activity was sorted prior to beginning recording sessions using an online sorting application (Sort Client, Plexon). Channel-level activity (Chestek et al., 2011) was defined using Sort Client's autothreshold procedure to set each channel threshold to 5.5 SDs from the mean signal amplitude. See Supplemental Experimental Procedures for details.

Behavioral Tasks and Training

Center-Out Task

Subjects performed a self-paced delayed center-out reaching task to eight targets (Figures 1C–1E). Trials were initiated by moving to the central target. A successful trial required a short hold at the center, moving to the peripheral target within a specified time, and a brief hold at the target. Successful trials resulted in a liquid reward; failed trials were repeated. Target directions were presented in a blocked pseudorandomized order. Subjects were overtrained in the center-out task performed with arm movements (MC) before starting BMI. In MC, the subject's arm moved in a KINARM exoskeleton (BKIN Technologies) that restricted movements to the horizontal plane (Figure 1C). See Supplemental Experimental Procedures for further details.

BMI-Force Simultaneous Control

The simultaneous control task (Figures 5A and 5B) required monkey J to perform an isometric force generation task with his arm at the same time as performing a center-out task under BMI control. A force sensor (Measurement Specialties) was placed within the primate behavioral chair. The force registered by the sensor was mapped to the size of a circular cursor on the display ("force cursor"). Target forces were presented as a circular ring ("force target"). The subject initialized BMI-SC trials by acquiring the force target, triggering the appearance of the BMI cursor and center target. The subject then had to complete a center-out reach with the BMI cursor while maintaining an applied force within the target range. If at any time the subject applied forces outside of the target range, an error occurred, causing the BMI cursor and task to disappear and the trial to be repeated.

One subject (monkey J) performed the BMI-SC task. BMI-SC was tested intermittently throughout the course of BMI-only learning series (i.e., practice in BMI-only with a particular decoder or CLDA-modifications thereof). Monkey J performed the force task with his right arm. BMI decoders for BMI-SC sessions were driven by neural activity primarily from the contralateral (left) hemisphere. See Supplemental Experimental Procedures for full details.

Brain-Machine Interface Algorithms

Real-time BMI control was implemented using a position-velocity KF (Wu et al., 2003; Kim et al., 2008; Gilja et al., 2012; Orsborn et al., 2012). The KF assumes two linear models:

$$x_{t+1} = Ax_t + w_t \qquad \text{(Equation 1)}$$

$$y_{t+1} = Cx_t + q_t, \qquad \text{(Equation 2)}$$

where x_t and y_t are the cursor state and neural activity at time t, respectively. Equation 1 represents the state-transition model, describing the evolution of the cursor state in time, and is specified by state-transition matrix A and additive Gaussian noise $wt \sim N(0, W)$. Equation 2 defines the relationship between neural activity and cursor state (the observation model) and is parameterized by the observation matrix C and additive Gaussian noise $q_t \sim N(0, Q)$.

A position-velocity KF was used, with the state variable defined to include cursor position (p) and velocity (v) in Cartesian space (see Supplemental Experimental Procedures for further details). Neural input to the KF (y_t) was defined as the firing rate of BMI units, estimated in nonoverlapping 100 ms bins. BMI ensembles typically included tens of units (range, 11–23; mean and mode, 16). For monkey J who performed BMI with channel-level activity, channel firing rates were scaled (mean subtracted, multiplied by a scaling factor) before being input to the KF to compensate for day-to-day variability in channels' statistical properties (see Supplemental Experimental Procedures).

With the KF matrices [A, W, C, and Q] defined, cursor movement is recursively estimated combining the state- and observation-based estimates. Equations for iterative estimation can be found elsewhere (Wu et al., 2003).

Decoder Training and Closed-Loop Decoder Adaptation Algorithms

Initial decoder parameters were trained via maximum-likelihood estimation. Training data were typically collected using a visual feedback protocol where subjects passively observed a cursor move through the center-out task. A small number of sessions tested other initialization methods. No qualitative behavioral or neural differences were found across series with different initialization methods, and our analyses do not distinguish between methods. See Supplemental Experimental Procedures for further information.

CLDA was performed using the SmoothBatch (Orsborn et al., 2012) and Re-FIT (Gilja et al., 2012) algorithms for monkey J and S, respectively. These algorithms use knowledge of task goals (i.e., reaching targets) to infer a subject's intent. The intended kinematics and observed neural activity during closed-loop BMI were used to re-estimate KF parameters. The SmoothBatch algorithm only re-estimated the observation model of the KF (matrices C and Q) and updates were constrained to enforce smoothness (Dangi et al., 2013). Re-FIT re-calculated all KF parameters. Algorithm details can be found in Orsborn et al. (2012) and Gilja et al. (2012).

In the two-learner paradigm, CLDA was used for two primary purposes: (1) to improve closed-loop performance from the initial decoder, and (2) to maintain performance in the event of shifts in neural activity (e.g., loss of a unit within the BMI ensemble). Initial CLDA was typically run for 5–15 min, to provide the subject with adequate performance to allow successful reaches to all targets. Midseries CLDA was performed if units were lost, or if the experimenter observed a drop in performance (typically due to instability in the recorded BMI ensemble; assessed in the session as a difference in success rate exceeding approximately 10%–20%). In this instance, CLDA was run for a very brief time (3–5 min, corresponding to one batch in Re-FIT and one to two updates in SmoothBatch). The goal was to compensate for neural activity changes to restore performance. BMI decoder parameters were remarkably stable across series, with the majority of changes occurring in the initial CLDA period (Figures S2I–S2K).

During a decoder series, the subjects performed BMI with a single decoder (or CLDA-updated versions thereof). Subjects also performed occasional blocks of manual control and/or visual observation. See Supplemental Experimental Procedures for further details. Table S1 summarizes all series used (decoder seed, length, number of CLDA sessions).

For daily retraining sessions (Figure S1), SmoothBatch CLDA was used to train a new decoder starting from different initial decoders using different (but overlapping) neural ensembles each day. Initial decoders were created using several different training methods (see Supplemental Experimental Procedures). CLDA was run until behavioral performance began to saturate (i.e., with the aim to improve performance as much as possible). Full details of the methods and data set for monkey S can be found elsewhere (Orsborn et al., 2012).

Data Analysis

Decoder series had varying lengths, initial performance, and final performance. As such, all comparisons focus on changes within-series. To quantify behavioral changes over time, all series (monkey S: 6, monkey J: 13) were used. Note that five series from monkey J overlap with data presented for the BMI-SC task. For analysis of neural changes associated with learning, we restricted our analysis to series lasting 3 or more days in which the subject used the same decoder for 2 days or more with no CLDA (monkey S: 4, monkey J: 10). This allowed us to better isolate changes in performance linked to neural adaptation, as opposed to CLDA. Inclusion of all series in neural analyses did not change any reported trends. Series length was also included as a potential factor in correlation analyses (Table S2).

Behavioral Metrics

Behavior was quantified using both task-performance metrics and measures of trajectory kinematics. Task performance was quantified by the percentage of trials that were correctly completed ("percent correct"), and the rate of successful trial completion ("success rate"). Because the task was self-paced, success rate and percent correct provide related, but different information about task proficiency. Reach kinematics were quantified by calculating the average movement error of trajectories. See Supplemental Experimental Procedures for further details on metric calculations.

To control for variability in the number of trials completed each day, and motivation changes across sessions, behavioral metrics were calculated using the first 300 trials performed within a day. Analysis using all trials completed in a series did not qualitatively change any reported results.

Directional Tuning

Unit directional tuning was computed by relating the mean firing rate with movement direction (Georgopoulos et al., 1986). Each unit's firing rate was fit to a cosine direction tuning function. The cosine fit was then used to estimate each unit's modulation depth (MD^U) and preferred direction (PD^U). See Supplemental Experimental Procedures for details. We use the superscript "U" to denote tuning properties for units to differentiate from tuning of the decoder (see below). Unit firing rates were estimated using nonoverlapping 100 ms bins (to match the decoding bin width). Tuning parameters were estimated using the average firing rate immediately surrounding the go-cue (100 ms prior, to 200 ms after) to capture the firing associated with reach initiations. Reach angle was determined by the reach target location. Selecting different time windows for firing rate estimation had no qualitative change on the presented results. Tuning parameters and their 95% confidence intervals (CIs) were estimated via linear regression in Matlab. All successfully initiated trials were used for tuning estimation. Units were said to be significantly direction tuned if the linear regression was statistically significant ($p < 0.05$). For nontuned units, MD^U was defined as 0, and PD^U was said to be undefined.

Quantifying Learning-Related Changes

To assess learning-related changes in neural activity, series were divided into "early," "middle," and "late" periods based on behavioral criteria. Behavior was quantified using three metrics: task percent correct, task success rate, and movement error. "Late" learning was characterized by performance within 20% of the best performance achieved during the series. "Early" learning periods were defined as all days in which performance was within 20% of the performance on day 1, and prior to the onset of the "late" phase. These thresholds had to be satisfied for all three behavioral metrics. Midlearning were all days in between early and late. In the rare event no days satisfied the late criterion, late days were defined as those days where the majority of behavior metrics met the "late" criteria. In typical series, "early" was day 1 only, and "late" was the last 2–3 days.

Changes in neural activity during a series were quantified by comparing unit tuning parameters (MD^U and PD^U) early and late in a series. For units that were not tuned or were not part of the BMI ensemble for the full series, changes were estimated using the first and last days when their tuning properties were well defined (see Supplemental Experimental Procedures). Changes in PD^U and MD^U were said to be significant if the 95% CI estimates of the two parameters did not overlap. For MD, both absolute and relative change ($\Delta MD^U_{rel} = 100(MD^{U,\,late} - MD^{U,\,early})/MD^{U,\,early}$), the latter reducing the dependence on absolute firing rates of units, were calculated.

Ensemble Tuning Maps

Ensemble-level changes in directional tuning were also quantified by comparing tuning "maps" over the series. A map consists of the fitted tuning curves for the BMI ensemble on a given day. To isolate changes in MD^U and PD^U, the baseline firing rate was subtracted from tuning curve fits. Pairwise correlations of daily maps allowed us to assess the similarity of ensemble tuning over time. Maps were computed using only units that were part of the ensemble across the entire series. The average similarity of a given day's map to all others (excluding self-comparison) was used to depict the time course of map changes (e.g., Figure 3F). The average correlation of the initial map with all others also captures the magnitude of change—in

both MD^U and PD^U tuning parameters—that occurred during the series (Figures 4A and 4B).

Neural Timing Analyses

To assess changes in neural recruitment timing, we quantified the time at which neurons became directionally tuned and the time of peak firing. Firing rates were estimated using 25 ms nonoverlapping bins. Tuning curves were fit using the firing rate of single bins, from 250 ms before to 500 ms after the go-cue. The onset time of tuning was defined as the first time when four consecutive bins produced statistically significant directional tuning fits ($p < 0.05$). Similar results were found with different criteria (number of consecutive bins, significance threshold). To calculate peak firing rate, trial-averaged firing rates were computed, grouped by target direction. Peak firing each day was defined as the maximal deviation from baseline (estimated as the firing rate 750 ms to 500 ms prior to the go-cue). Only units with significant tuning "early" and "late" in learning where tested.

Decoder Tuning Parameters

To assess differences between decoder parameters and neural activity, we quantified the directional tuning of the decoder. The KF observation model can be viewed as defining position- and velocity-based cosine-tuning models for each unit. We used the decoder parameters in C to compute the position- and velocity-based MD and PD for each unit, defining both properties in a similar fashion as for units. We use the superscripts "C_v" and "C_p" to denote the decoder's velocity- and position-based tuning parameters, respectively (e.g., MD^{Cv} indicates the KF's velocity MD). Further definition of these parameters can be found in the Supplemental Experimental Procedures.

Decoder and unit tuning properties were compared to assess whether decoder properties influenced neural adaptation. PD mismatch between units and the decoder was quantified by computing the difference between the decoder's PD and the unit's PD (estimated via neural activity) on day 1 of a series. Relationships between decoder and unit MDs were assessed using a unit's average MD across all decoders used in a series.

SUPPLEMENTAL INFORMATION

Supplemental Information includes Supplemental Experimental Procedures, four figures, and three tables and can be found with this article online at http://dx.doi.org/10.1016/j.neuron.2014.04.048.

ACKNOWLEDGMENTS

This work was supported by the American Heart Association predoctoral fellowship (to A.L.O.), the National Science Foundation Graduate Research Fellowship (to H.G.M.), the Defense Advanced Research Projects Agency contract N66001-10-C-2008 (to J.M.C.), and the National Science Foundation grants CBET-0954243 and EFRI-M3C 1137267 (to J.M.C.). We thank E. Rich for surgical assistance.

Accepted: April 18, 2014
Published: June 18, 2014

REFERENCES

Carmena, J.M. (2013). Advances in neuroprosthetic learning and control. PLoS Biol. *11*, e1001561.

Carmena, J.M., Lebedev, M.A., Crist, R.E., O'Doherty, J.E., Santucci, D.M., Dimitrov, D.F., Patil, P.G., Henriquez, C.S., and Nicolelis, M.A.L. (2003). Learning to control a brain-machine interface for reaching and grasping by primates. PLoS Biol. *1*, E42.

Chase, S.M., Kass, R.E., and Schwartz, A.B. (2012). Behavioral and neural correlates of visuomotor adaptation observed through a brain-computer interface in primary motor cortex. J. Neurophysiol. *108*, 624–644.

Chestek, C.A., Gilja, V., Nuyujukian, P., Foster, J.D., Fan, J.M., Kaufman, M.T., Churchland, M.M., Rivera-Alvidrez, Z., Cunningham, J.P., Ryu, S.I., and Shenoy, K.V. (2011). Long-term stability of neural prosthetic control signals from silicon cortical arrays in rhesus macaque motor cortex. J. Neural Eng. *8*, 045005.

Collinger, J.L., Wodlinger, B., Downey, J.E., Wang, W., Tyler-Kabara, E.C., Weber, D.J., McMorland, A.J., Velliste, M., Boninger, M.L., and Schwartz, A.B. (2013). High-performance neuroprosthetic control by an individual with tetraplegia. Lancet *381*, 557–564.

Dangi, S., Orsborn, A.L., Moorman, H.G., and Carmena, J.M. (2013). Design and analysis of closed-loop decoder adaptation algorithms for brain-machine interfaces. Neural Comput. *25*, 1693–1731.

Danziger, Z., Fishbach, A., and Mussa-Ivaldi, F.A. (2009). Learning algorithms for human-machine interfaces. IEEE Trans. Biomed. Eng. *56*, 1502–1511.

Fetz, E.E. (2007). Volitional control of neural activity: implications for brain-computer interfaces. J. Physiol. *579*, 571–579.

Foldes, S.T., and Taylor, D.M. (2013). Speaking and cognitive distractions during EEG-based brain control of a virtual neuroprosthesis-arm. J. Neuroeng. Rehabil. *10*, 116.

Ganguly, K., and Carmena, J.M. (2009). Emergence of a stable cortical map for neuroprosthetic control. PLoS Biol. *7*, e1000153.

Ganguly, K., Dimitrov, D.F., Wallis, J.D., and Carmena, J.M. (2011). Reversible large-scale modification of cortical networks during neuroprosthetic control. Nat. Neurosci. *14*, 662–667.

Georgopoulos, A.P., Schwartz, A.B., and Kettner, R.E. (1986). Neuronal population coding of movement direction. Science *233*, 1416–1419.

Gilja, V., Nuyujukian, P., Chestek, C.A., Cunningham, J.P., Yu, B.M., Fan, J.M., Churchland, M.M., Kaufman, M.T., Kao, J.C., Ryu, S.I., and Shenoy, K.V. (2012). A high-performance neural prosthesis enabled by control algorithm design. Nat. Neurosci. *15*, 1752–1757.

Golub, M.D., Yu, B.M., and Chase, S.M. (2012). Internal models engaged by brain-computer interface control. Conf. Proc. IEEE Eng. Med. Biol. *2012*, 1327–1330.

Green, A.M., and Kalaska, J.F. (2011). Learning to move machines with the mind. Trends Neurosci. *34*, 61–75.

Hwang, E.J., Bailey, P.M., and Andersen, R.A. (2013). Volitional control of neural activity relies on the natural motor repertoire. Curr. Biol. *23*, 353–361.

Jackson, A., and Fetz, E.E. (2011). Interfacing with the computational brain. IEEE Trans. Neural Syst. Rehabil. Eng. *19*, 534–541.

Jarosiewicz, B., Chase, S.M., Fraser, G.W., Velliste, M., Kass, R.E., and Schwartz, A.B. (2008). Functional network reorganization during learning in a brain-computer interface paradigm. Proc. Natl. Acad. Sci. USA *105*, 19486–19491.

Jarosiewicz, B., Masse, N.Y., Bacher, D., Cash, S.S., Eskandar, E., Friehs, G., Donoghue, J.P., and Hochberg, L.R. (2013). Advantages of closed-loop calibration in intracortical brain-computer interfaces for people with tetraplegia. J. Neural Eng. *10*, 046012.

Kim, S.-P., Simeral, J.D., Hochberg, L.R., Donoghue, J.P., and Black, M.J. (2008). Neural control of computer cursor velocity by decoding motor cortical spiking activity in humans with tetraplegia. J. Neural Eng. *5*, 455–476.

Koralek, A.C., Jin, X., Long, J.D., 2nd, Costa, R.M., and Carmena, J.M. (2012). Corticostriatal plasticity is necessary for learning intentional neuroprosthetic skills. Nature *483*, 331–335.

Koralek, A.C., Costa, R.M., and Carmena, J.M. (2013). Temporally precise cell-specific coherence develops in corticostriatal networks during learning. Neuron *79*, 865–872.

Li, Z., O'Doherty, J.E., Lebedev, M.A., and Nicolelis, M.A.L. (2011). Adaptive decoding for brain-machine interfaces through Bayesian parameter updates. Neural Comput. *23*, 3162–3204.

Merel, J., Fox, R., Jebara, T., and Paninski, L. (2013). A multi-agent control framework for co-adaptation in brain-computer interfaces. C.J.C. Burges, L. Bottou, Z. Ghahramani, and K.Q. Weinberger, eds. Proceedings of the 26th Annual Conference on Neural Information Processing Systems, 2841–2849.

Musallam, S., Corneil, B.D., Greger, B., Scherberger, H., and Andersen, R.A. (2004). Cognitive control signals for neural prosthetics. Science *305*, 258–262.

Orsborn, A.L., Dangi, S., Moorman, H.G., and Carmena, J.M. (2012). Closed-loop decoder adaptation on intermediate time-scales facilitates rapid BMI performance improvements independent of decoder initialization conditions. IEEE Trans. Neural Syst. Rehabil. Eng. *20*, 468–477.

Shanechi, M.M., and Carmena, J.M. (2013). Optimal feedback-controlled point process decoder for adaptation and assisted training in brain-machine interfaces. 6th International IEEE/EMBS Conference on Neural Eng. 653–656.

Suminski, A.J., Tkach, D.C., and Hatsopoulos, N.G. (2009). Exploiting multiple sensory modalities in brain-machine interfaces. Neural Netw. *22*, 1224–1234.

Suminski, A.J., Tkach, D.C., Fagg, A.H., and Hatsopoulos, N.G. (2010). Incorporating feedback from multiple sensory modalities enhances brain-machine interface control. J. Neurosci. *30*, 16777–16787.

Taylor, D.M., Tillery, S.I., and Schwartz, A.B. (2002). Direct cortical control of 3D neuroprosthetic devices. Science *296*, 1829–1832.

Velliste, M., Perel, S., Spalding, M.C., Whitford, A.S., and Schwartz, A.B. (2008). Cortical control of a prosthetic arm for self-feeding. Nature *453*, 1098–1101.

Wander, J.D., Blakely, T., Miller, K.J., Weaver, K.E., Johnson, L.A., Olson, J.D., Fetz, E.E., Rao, R.P.N., and Ojemann, J.G. (2013). Distributed cortical adaptation during learning of a brain-computer interface task. Proc. Natl. Acad. Sci. USA *110*, 10818–10823.

Wu, W., Black, M.J., Gao, Y., Bienenstock, E., Serruya, M., Shaikhouni, A., and Donoghue, J.P. (2003). Neural decoding of cursor motion using a Kalman filter. Proceedings of the 15th Annual Conference on Neural Information Processing Systems. 133–140.